AGU PUBLICATIONS

Geophysical Research Letters

RESEARCH LETTER
10.1002/2016GL069792

Key Points:
- The July OLR field over Africa is correlated 0.75 with named Atlantic storms, 1979–2015
- Hindcast predictions of named Atlantic storms based on July OLR succeed 87% of years 2001–2015
- OLR predictors are statistically robust, highly detectable, and physically linked to the predictand

Supporting Information:
- Supporting Information S1

Correspondence to:
K. B. Karnauskas,
kristopher.karnauskas@colorado.edu

Citation:
Karnauskas, K. B., and L. Li (2016), Predicting Atlantic seasonal hurricane activity using outgoing longwave radiation over Africa, *Geophys. Res. Lett.*, *43*, 7152–7159, doi:10.1002/2016GL069792.

Received 27 MAY 2016
Accepted 20 JUN 2016
Accepted article online 21 JUN 2016
Published online 8 JUL 2016

Predicting Atlantic seasonal hurricane activity using outgoing longwave radiation over Africa

Kristopher B. Karnauskas[1] and Laifang Li[2]

[1]Department of Atmospheric and Oceanic Sciences and Cooperative Institute for Research in Environmental Sciences, University of Colorado Boulder, Boulder, Colorado, USA, [2]Department of Physical Oceanography, Woods Hole Oceanographic Institution, Woods Hole, Massachusetts, USA

Abstract Seasonal hurricane activity is a function of the amount of initial disturbances (e.g., easterly waves) and the background environment in which they develop into tropical storms (i.e., the main development region). Focusing on the former, a set of indices based solely upon the meridional structure of satellite-derived outgoing longwave radiation (OLR) over the African continent are shown to be capable of predicting Atlantic seasonal hurricane activity with very high rates of success. Predictions of named storms based on the July OLR field and trained only on the time period prior to the year being predicted yield a success rate of 87%, compared to the success rate of NOAA's August outlooks of 53% over the same period and with the same average uncertainty range (±2). The resulting OLR indices are statistically robust, highly detectable, physically linked to the predictand, and may account for longer-term observed trends.

1. Introduction

Despite the obvious human and economic impact of tropical cyclones, predicting how active an upcoming (or ongoing) Atlantic hurricane season will be remains a formidable challenge. Since the U.S. National Oceanic and Atmospheric Administration (NOAA) National Hurricane Center (NHC) and Climate Prediction Center (CPC) began issuing bounded predictions in 2001 (i.e., "6–10 Named Storms"), the success rate of such predictions issued in early August has been 53% (Table 1). In other words, the actual number of named storms fell within the predicted range in 8 of the 15 years from 2001 through 2015—with a priori knowledge of the number of named storms in the first 2 months of the official Atlantic hurricane season.

Despite how 53% may sound, such a success rate is in fact evidence of real forecast skill. Given 15 ± 5 named Atlantic storms (mean ± standard deviation) per year from 2001 through 2015, and a lag-1 autocorrelation coefficient of −0.10, persistence-based methods would naturally have yielded inferior success rates (Table 1). Straight persistence (i.e., the prior year's outcome ± 2) would have yielded a 33% success rate, and the prior 7 year mean (±2) would have yielded a success rate of 47%—in terms of named storms. In addition to named storms, NOAA's seasonal outlooks include predictions of subgroups and derivatives thereof such as hurricanes, major hurricanes, and accumulated cyclone energy (ACE), which have yielded success rates of 53%, 67%, and 53%, respectively. Predictions of ACE based on straight persistence and the prior 7 year mean would have yielded success rate of 33%. Moreover, impressive progress appears to have been made; seven of the eight successful early-August predictions of named storms by NOAA occurred in the last 9 years (2007–2015). Nonetheless, there is clearly room for improvement in the science and art of seasonal hurricane prediction, from which many sectors of society may benefit.

Probabilistic predictions of Atlantic seasonal hurricane activity (such as those issued by NOAA in late May and early August) are typically based on a blend of observations and model forecasts of several atmospheric and oceanic parameters over the tropical Atlantic including sea surface temperature (SST), humidity, vorticity, and vertical wind shear, as well as characteristics of remote climatic phenomena such as the El Niño–Southern Oscillation (ENSO) and west African monsoon [see *Bell and Chelliah*, 2006, and references therein]. However, seasonal hurricane predictions at NOAA are not derived strictly from numerical inputs; the former parameters are considered guidance. and the human element takes the form of expert judgment. *Karnauskas* [2006] explored the potential association between Atlantic seasonal hurricane activity and the meridional gradient of outgoing longwave radiation (OLR) across Africa using satellite

Table 1. Predicted and Actual Named Storms and Accumulated Cyclone Energy (ACE) Over Time[a]

	Named Storms		ACE Index	
Year	NHC	Actual	NHC	Actual
1994		7		32
1995		19		228
1996		13		166
1997		8		41
1998		14		182
1999		12		177
2000		15		119
2001	9–12	15	**86–120**	**110**
2002	7–10	12	**52–86**	**67**
2003	12–15	16	103–146	176
2004	**12–15**	**15**	79–131	227
2005	18–21	28	158–236	250
2006	12–15	10	96–149	79
2007	**13–16**	**15**	123–175	74
2008	**14–18**	**16**	**123–201**	**146**
2009	**7–11**	**9**	**53–96**	**53**
2010	**14–20**	**19**	**149–228**	**165**
2011	**14–19**	**19**	**125–199**	**126**
2012	12–17	19	69–125	129
2013	**13–19**	**14**	111–176	36
2014	**7–12**	**8**	**37–83**	**67**
2015	6–10	11	**23–65**	**63**

[a]Predicted ranges of and actual named atlantic storms and Accumulated Cyclone Energy (ACE) since 2001, when NOAA began issuing bounded predictions of both. Actuals since 1994 are also shown to include the data pertaining to comparisons to predictions based on persistence and the prior 7 year mean as discussed in the main text. The NOAA predictions shown here were issued in early August of the year indicated (the official Atlantic hurricane season spans June through November). Bold type indicates successful predictions; the success rate of NOAA predictions issued in early August for named storms and ACE is 53%.

observations between 1982 and 2004 (23 years). The OLR gradient was argued to be an integrative quantity reflecting the intensity of the Intertropical Convergence Zone (ITCZ) over Sahel Africa related to the production of easterly waves, as well as the meridional temperature gradient related to the African easterly jet (AEJ) via the thermal wind relation. A similar concept has also been applied recently to storm-by-storm and monthly correlations, yielding promising results [*Price et al.*, 2015]. Here we further exploit such mechanistic relationships between the meridional structure of the OLR field over Africa and Atlantic seasonal hurricane activity using observations between 1979 and 2015 (37 years), build robust statistical models based on observed relationships, and explicitly evaluate the performance of those models in hindcast mode relative to seasonal predictions issued by NOAA as well as the Colorado State University (CSU) Tropical Meteorology Project since 2001.

2. Data

In this study, we utilize several monthly, gridded observational data sets, focusing on the period of January 1979 through December 2015, including the following:

1. NOAA Interpolated OLR, 2.5° resolution [*Liebmann and Smith*, 1996].
2. Global Precipitation Climatology Project version 2.2 precipitation, 2.5° resolution [*Adler et al.*, 2003].
3. NASA Goddard Institute for Space Studies (GISS) surface temperature (GISSTemp), 2° resolution with 250 km smoothing [*Hansen et al.*, 2010].
4. NASA GISS surface temperature merged with NOAA Extended Reconstructed Sea Surface Temperature version 4, 2° resolution with 1200 km smoothing (GISSTemp + ERSSTv4) [*Hansen et al.*, 2010].
5. National Centers for Environmental Prediction/National Center for Atmospheric Research Reanalysis [*Kalnay et al.,* 1996] relative humidity, horizontal wind, and tropopause temperature for calculating the hurricane genesis potential index (GPI; see Appendix A for details).

In addition, we utilize monthly climate indices defining the El Niño–Southern Oscillation (ENSO) and the Atlantic Multidecadal Oscillation (AMO) provided by the NOAA Earth System Research Laboratory (ESRL), Physical Sciences Division (PSD), historical Atlantic tropical storm statistics from the NOAA NHC and Hurricane Research Division (HRD), and historical Atlantic tropical storm predictions archived by the NOAA Climate Prediction Center (CPC) and the Colorado State University (CSU) Tropical Meteorology Project. Tropical cyclone tracks from 1979 to 2014 were gathered from the HURricane DATa second generation (HURDAT2) [*Landsea and Franklin*, 2013) data set. A statement on data availability including Web addresses for all of the above data sets is provided below in the Acknowledgments section and section 2.

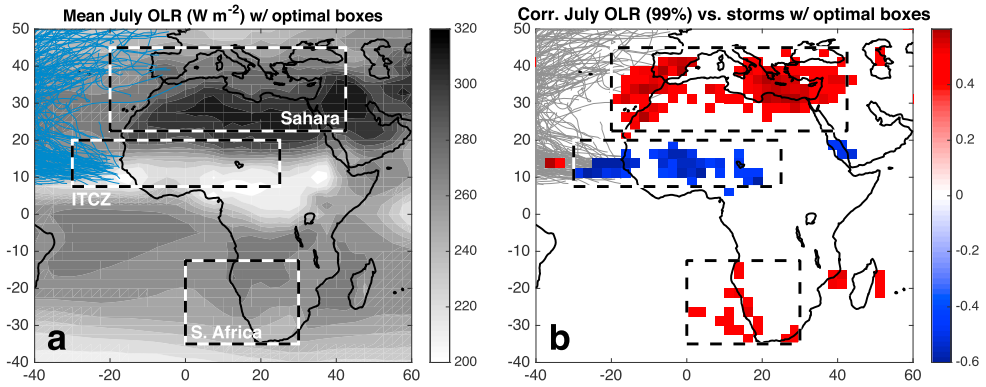

Figure 1. (a) Climatological OLR (W m^{-2}) during July 1979–2015. (b) Significant correlations (99%) between July OLR and the number of named Atlantic storms, 1979–2015. The dashed boxes in both panels indicate the OLR indices referred to in the main text and used in subsequent figures. Tracks from all 556 tropical cyclones, 1979–2014, from the HURDAT2 data set are shown in both panels.

3. Optimal OLR Index

The climatological distribution of OLR over Africa (Figure 1a) reveals strong meridional gradients between the very high OLR (~310 W m^{-2}) over northern Africa due to the hot and cloud-free Sahara Desert, very low OLR (~210 W m^{-2}) over central Africa due to the Intertropical Convergence Zone (ITCZ), and moderately high OLR (~270 W m^{-2}) over southern Africa—also due to a region of strong descent within the global Hadley circulation. We seek to develop a skillful OLR-based predictor for Atlantic seasonal hurricane activity that can be made available in early August (synchronized with the updated NOAA and CSU predictions); thus, we focus on the July mean OLR fields. The correlation between July OLR at every location and the number of named Atlantic storms between 1979 and 2015 (Figure 1b) reveals a coherent tripole structure involving all three of the aforementioned features of the climatological OLR distribution over Africa. Active Atlantic hurricane seasons are associated with a strengthened and poleward-shifted climatological OLR pattern including higher OLR along the northern edge of Africa and southern Europe, lower OLR across the Sahel or northern edge of the ITCZ, and higher OLR over southern Africa. The swath of negative correlation across the Sahel is closely aligned with a pronounced region of tropical cyclogenesis just offshore of West Africa, as indicated by HUDAT2 tracks. Qualitatively, similar results are obtained by correlating the July OLR with ACE (Figure S3a in the supporting information).

The time evolution of "optimal" July OLR indices over the Sahara, ITCZ, and southern Africa (i.e., box-averages encompassing the regions of highly significant correlations shown in Figure 1b) is shown in Figure 2a, along with a single OLR index combining the three boxes in Figure 2b. The combined OLR index is computed as simply the average of the normalized OLR indices over the Sahel and southern Africa minus the normalized OLR index over the ITCZ. The correlation between the July OLR index and the number of named Atlantic storms from 1979 to 2015 is 0.75, which is clearly statistically significant (99%). For comparison, correlations between named Atlantic storms and the AMO index in July and the NINO3.4 index in the following December–February season (which presumes the availability of an accurate ENSO forecast) are significant but lower than that with the OLR index (Figure 2c). Some of the correlation between the above-mentioned variables and named Atlantic storms may be due to linear trends present over 1979–2015; detrending reduces the correlation coefficient by 29% for AMO, but only by 9% for the combined OLR index.

The correlation between the July OLR index and the number of named Atlantic storms reported here (0.75) is higher than that of *Karnauskas* [2006]—partly due to the continued strong association between African OLR and named Atlantic storms over the subsequent decade and partly due to updated data and methods. In terms of developing the OLR predictors, there are three main differences in the data and methodology between the present study and *Karnauskas* [2006]. (1) The period of analysis has been expanded from 23 years (1982–2004) to 37 years (1979–2015). (2) The two original boxes (Sahara and ITCZ) have been moved slightly based on the observed covariability between the seasonal OLR fields and the

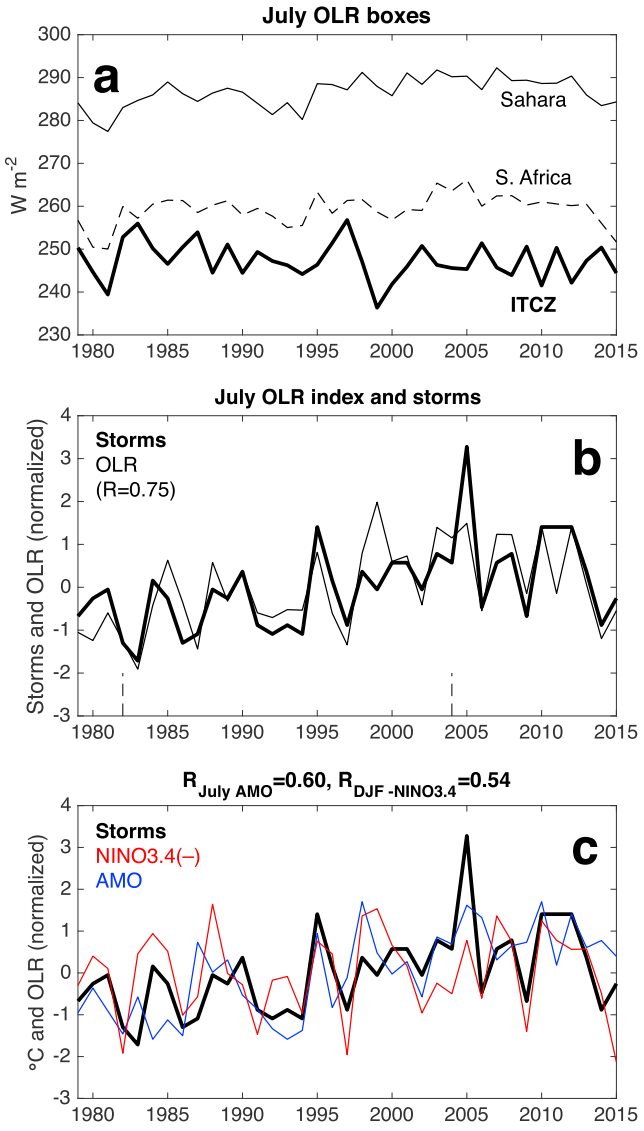

Figure 2. (a) Time series of individual box-averaged July OLR indices (W m^{-2}) noted in Figure 1. (b) July OLR index (thin line) and the number of named Atlantic storms (heavy line) (both time series normalized to facilitate comparison). (c) Number of named Atlantic storms (black), NINO3.4 index (red), and AMO index (blue) (all time series normalized). The dashed lines in Figure 2b denote the period of analysis in *Karnauskas* [2006].

time series of named storms; the boxes in *Karnauskas* [2006] were simply based on the annual mean climatology. (3) A third box over southern Africa has been added to exploit the remote covariability provided by the Hadley circulation. The statistical robustness of the spatial pattern in Figure 1b, its temporal evolution (Figure 2b), and the three-box index that quantifies it is further confirmed by empirical orthogonal function (EOF) analysis (Figure S1); the correlation between the July combined OLR index and the second principal component of July OLR is 0.97.

The meridional structure of the OLR field over Africa is a reflection of the intensity of both the ascending motion within the Sahelian ITCZ and the subtropical descending motion over the Sahara and southern Africa, which is itself an important regional center of action embedded within the global Hadley circulation [*Karnauskas and Ummenhofer*, 2014] and related to the Indian monsoon through a Rossby wave response [*Rodwell and Hoskins*, 1996]. Indeed, composite and regression analyses highlighting the large-scale spatial patterns of OLR variability associated with variability in Atlantic seasonal hurricane activity (Figures 3a and 3b), along with the objective EOF analysis (Figure S1), robustly show that these three centers of action vary in concert and project strongly onto the regional Hadley cell paradigm. In contrast, precipitation alone only captures variability of the ITCZ (Figures 3c and 3d), as climatological rainfall within the subtropical descent regions is near zero and thus contains no useful signal despite the important circulation changes detectable in OLR. Given that the subtropics are relatively dry, the OLR signal over the Sahara and southern Africa that is statistically related to Atlantic seasonal hurricane activity is being driven by surface temperature (Figures 3e and 3f), which is clearly an important element in setting up meridional temperature gradients that are dynamically linked to the AEJ and contribute to instabilities giving rise to easterly waves [*Hsieh and Cook*, 2008]. The meridional structure of OLR over Africa, it seems, is an ideal candidate predictor for Atlantic seasonal hurricane activity due to its robust, highly detectable signal and strong mechanistic connections to multiple factors known to influence tropical cyclone formation including the ITCZ, AEJ, easterly waves, and more generally the overall vigor of the atmosphere's overturning (Hadley) circulation just upstream of the main development region (MDR) [*Zhang and Wang*, 2013].

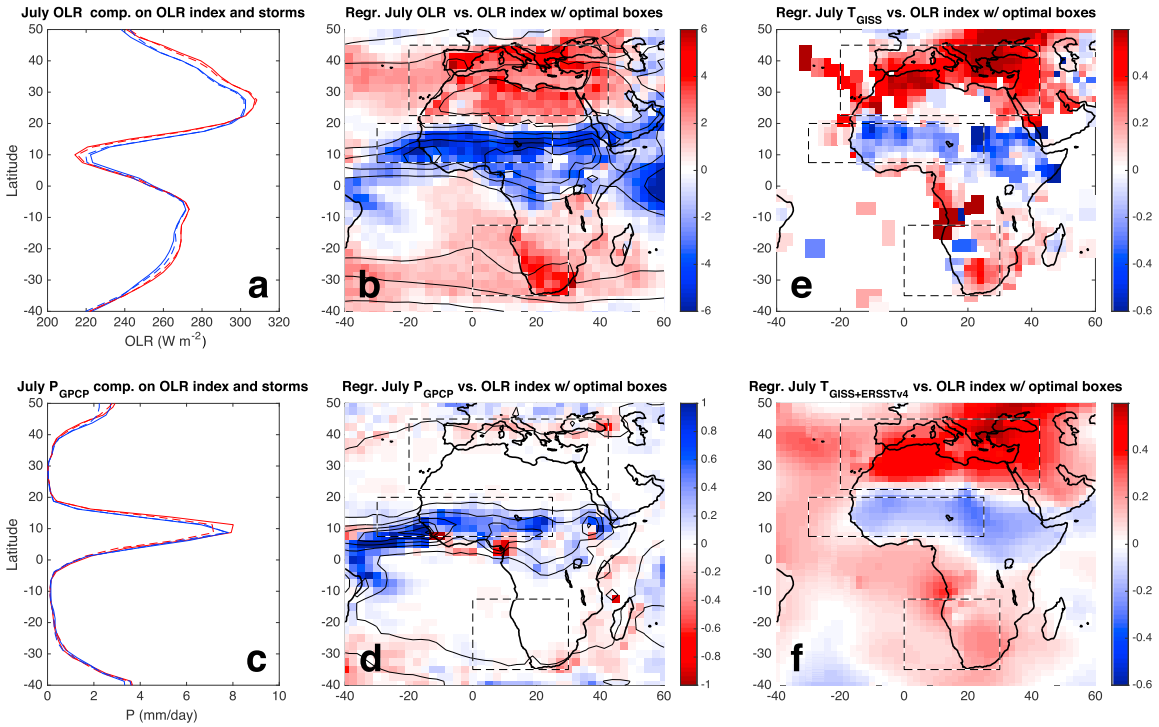

Figure 3. (a) Zonal mean (20°W–40°E) profiles of July OLR (W m^{-2}) composited onto the July OLR index (solid lines) and onto the number of named Atlantic storms (dashed lines). Positive (negative) composites are represented by red (blue) lines and represent the average of cases where the index is at least 1 standard deviation above (below) average. (b) Map of July OLR (W m^{-2}) regressed onto the July OLR index. (c and d) As in Figures 3a and 3b but for July precipitation (mm day^{-1}). (e) Map of July surface temperature (°C) from GISS regressed onto the July OLR index. (f) As in Figure 3e but for the smoother GISS product merged with ERSSTv4. The period of analysis for all six panels is 1979–2015.

4. Seasonal Predictability

The present section demonstrates the predictive skill of the OLR indices (July) developed in the previous section and compares their performance in predicting the number of named Atlantic storms with corresponding predictions issued in early August of each year since 2001 by NOAA and CSU. We employ two algorithms: simple multiple linear regression (MLR) and random forest prediction (RF; a machine learning technique). In both cases, the models are only trained on data prior to the year for which the prediction is being made. In other words, the prediction for 2001 is made with knowledge of OLR, storm counts, etc. only from 1979 to 2000. Prior to calculating the prediction for 2002, the models are retrained on data through 2001, and so on. Outputs of the numerical predictions are rounded to the nearest whole number (of storms). Identification of the optimal OLR indices used as predictors is not highly sensitive to the time period chosen; the correlation field shown in Figure 1b for the full period is very similar to the resulting field calculated using only the period of 1979–2000 (Figure S2). Finally, a prediction is considered successful if the actual number of named Atlantic storms (or ACE) falls within the predicted range.

The OLR-based predictions of named Atlantic storms made by the MLR technique were successful in 12 of the 15 years from 2001 through 2015, or a success rate of 80% (Figure 4a). Binary performance metrics such as success rate, as defined here, are clearly sensitive to the size of the range (i.e., the difference between the maximum and minimum predicted values). We therefore test the sensitivity of this result using three different uncertainty schemes for defining the size of the ranges. In one scheme (red), we permit the MLR calculation to determine the range in each year, but ensure that the 15 year average range is 4 (i.e., predicted value ±2) by fixing the confidence interval to the necessary value throughout the exercise (which happens to be 90%). In a second scheme (orange), we set the size of the range in each year equal to that of the NOAA prediction in the same year. Since 2001, the NOAA prediction ranges issued in early August have varied between 3 (e.g., "9–12 Named Storms" in 2001) and 6 (e.g., "14–20 Named Storms" in 2010), with a 15 year average range of 4, and typically with a stated confidence of around 70%. The third scheme (brown) simply assigns a constant range of 4 in each year (i.e., predicted value ±2). Under all three uncertainty schemes, the OLR-based predictions yielded a success rate of 80%,

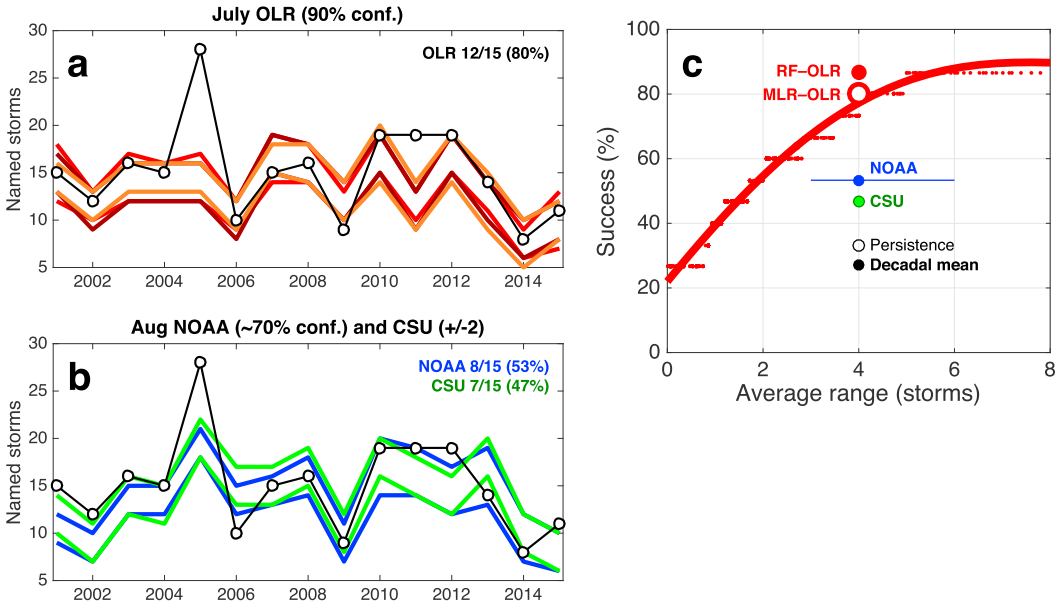

Figure 4. (a) Predicted number of named Atlantic storms based on July OLR (colored ranges) and the actual number of named Atlantic storms (black line with white circles). The red lines denote predictions with a variable range as determined by the regression procedure, but ending with an average range of 4 over the period of 2001–2015 (the same average range as the NOAA predictions). The orange lines denote predictions with a variable range equal to those of the NOAA predictions in each year. The brown lines denote predictions with a constant range of ±2 storms. (b) As in Figure 4a but for the August seasonal predictions by NOAA (blue) and CSU (green). (c) Success rate (% of years, 2001 through 2015, in which the actual number of named Atlantic storms fell within the predicted range) as a function of average range (±*N* storms) for predictions based on the annual number of named Atlantic storms averaged over the previous decade (filled black circle), persistence (the number of named Atlantic storms in the previous year; open black circle), CSU (green), NOAA (blue), and OLR (red).

as compared to the 53% success rate of the NOAA predictions, and the 47% success rate of CSU predictions since 2001 (Figure 4b; CSU predictions are issued without ranges; here we assign to them a constant range of 4, or predicted value ±2, to enable comparison). Predictions of ACE based solely on July OLR are on par with NOAA predictions thereof (53%), with a correlation between the July OLR index and ACE of 0.71 (Figures S3b and S3c).

We can further generalize the success rates achievable with the OLR indices and their dependence on the chosen range size by repeating predictions under the first of the aforementioned uncertainty schemes, but varying the confidence interval that remains fixed throughout the 15 predictions from 0.1% to 99.9% (or α from 0.999 to 0.001), resulting in 15 year average ranges from 0 (i.e., absolute precision but low confidence) to 8 (i.e., predicted value ±4 with very high confidence—arguably not a useful prediction). This sensitivity analysis (Figure 4c) indicates that the success rate of OLR-based predictions (MLR technique) varies from 27% for a forecast range of zero (i.e., pinpoint accuracy) to 53% for a forecast range of 2 (i.e., ±1 storm) to 87% for a forecast range of 6 (i.e., ±3 storms).

The RF predictions [*Breiman*, 2001] confirm the improved predictive skill using OLR-based predictors. In the RF prediction, we included eight predictors (combined OLR index; OLR in three individual boxes, July GPI in the MDR, July AMO, and DJF ENSO; and the number of pre-August named storms). Among them, the combined OLR index is ranked as the most important predictor according to the RF algorithm (Figure 5a). The importance factor of the combined OLR index is on average 1.2, but dropped to 1.0 for July GPI in the MDR (Figure 5a). Consistent with the importance factor, the RF predictions using the OLR-based indices achieve 87% success rate (13 out of 15; Figures 4c and 5c). The success rate decreases to 53% for the predictions without OLR (Figure 5d), exactly the same as the predictions by NOAA, in which the OLR-based predictors have not yet been formally implemented. It is noteworthy that the RF predictions using all eight predictors lead to lower success rate (73%) than the predictions using only OLR-based predictors (Figure 5b). The lower skill likely reflects an overfitting problem. The limited number of training samples (25–40) but large number of predictors can result in an artificially good fit for training samples but bad performance for validation samples. As a result, OLR-based predictors outperform the other predictors for Atlantic seasonal hurricane activity.

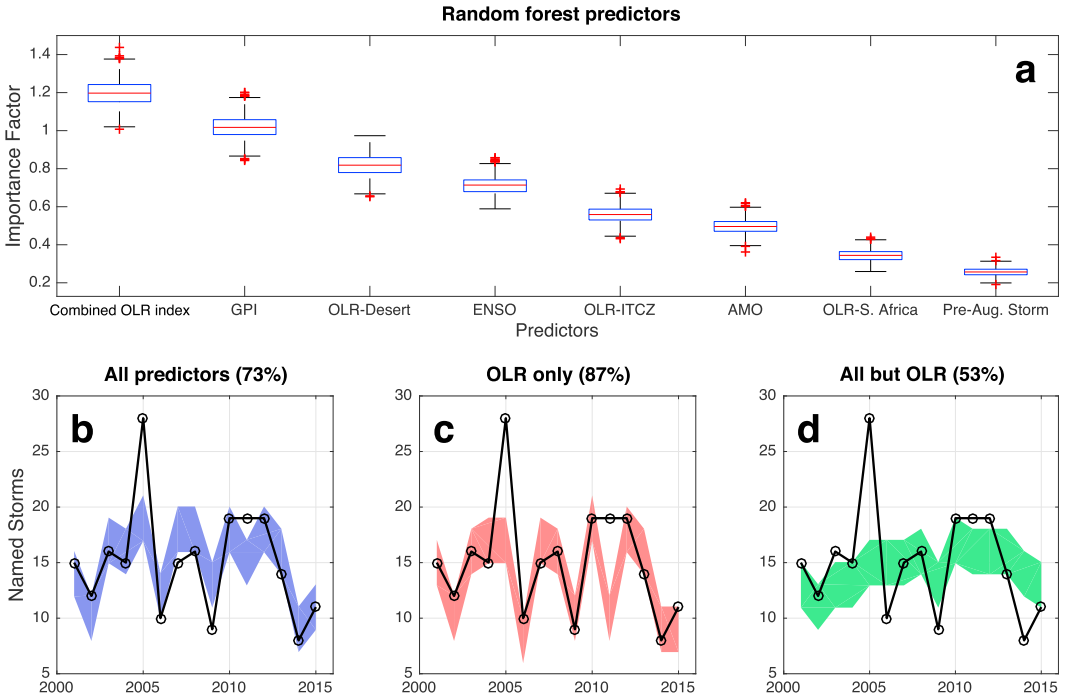

Figure 5. Random forest analysis of OLR and several other commonly utilized predictors including the genesis potential index (GPI), ENSO, AMO, and the number of named Atlantic storms prior to August. (a) Box and whisker plot showing the importance factor of each predictors according to 1000 iterations of RF algorithm. From the bottom to the top, the box-whisker plot shows the minimum, 25%; median, 75%; and maximum values of the importance factor. The red plus signs are the outlier samples. (b) RF prediction using all eight predictors shown in Figure 5a, (c) RF prediction using only OLR-based predictors, and (d) RF prediction without OLR. The shaded envelopes are ±2 ranges.

5. Summary and Discussion

A set of indices based solely upon satellite-derived OLR were developed and shown to be capable of predicting Atlantic seasonal hurricane activity with very high rates of success. The resulting OLR indices are statistically robust, highly detectable, and mechanistically linked to Atlantic seasonal hurricane activity. The physical connection between the OLR field over Africa and Atlantic seasonal hurricane activity is due to the meridional OLR gradient reflecting both the temperature gradient between the Sahara Desert and central Africa including the Gulf of Guinea, which drives the AEJ and the intensity of the ITCZ. Through the impact on AEJ intensity and ITCZ convection, the OLR index can be related to instabilities associated with easterly wave production [*Hsieh and Cook*, 2008]—some of which propagate across the West African coast into the tropical Atlantic region and further develop into tropical cyclones [*Thorncroft and Hodges*, 2001; *Hopsch et al.,* 2010].

In terms of predicting the number of named storms, the large difference in success rates between the OLR-based predictions (80–87%) and NOAA and CSU predictions (47-53%) is surprising, considering the simplicity of linear regression and the essentially univariate nature of the predictors compared to the diversity of data, models, and experience considered by the NOAA and CSU groups as illustrated in the discussion accompanying each outlook issued. Depending on the application or real-world context, if the tolerance for uncertainty was relatively small (e.g., within ±1 storm), the OLR-based predictors developed here would seem to offer such precision without sacrificing accuracy.

The primary benefit of OLR appears to be improved seasonal predictions of named storms made in early August, as the skill of OLR-based predictions of hurricanes, major hurricanes, and ACE is on par with the NOAA predictions, as is that of predictions of named storms based on the May OLR field. As May is prior to the start of the official Atlantic hurricane season, the skill of the May OLR field in predicting the upcoming hurricane season is likely due to the autocorrelation exhibited by OLR anomalies across the months leading up to—and into—the hurricane season. For example, the correlation coefficient between the May and June

OLR indices is 0.56, the correlation between the June and July OLR indices is 0.63, and the correlation between the July and June–November OLR indices is 0.84.

Finally, it is intriguing to consider whether the close association between the meridional structure of OLR across Africa and Atlantic seasonal hurricane activity extends beyond the interannual time scale. The linear trend in OLR over the analysis period (Figure S4a) projects strongly onto the spatial pattern of detrended OLR variability that is correlated with named storms and ACE (or OLR EOF2). Is the linear (or multidecadal) trend in the number of named Atlantic storms since 1979 associated with that of meridional OLR gradients over Africa? While some of the OLR trend appears to be driven by increasing surface temperatures (especially over northern Africa and southern Europe; Figure S4b), the ITCZ-related component of the OLR trend is not straightforward and deserves further attention [*Dong and Sutton*, 2015]. Nonetheless, the ongoing discussion surrounding the impact of multidecadal and anthropogenic climate change on tropical cyclones—typically centered on the environmental conditions within the MDR—should also consider the dynamical configuration upstream of the MDR (i.e., Africa), and OLR provides a diagnostic framework in which to do so.

Appendix A: Genesis Potential Index

The hurricane genesis potential index (GPI), which represents environmental conditions for hurricane genesis [*Emanuel and Nolan*, 2004], is also calculated as

$$\mathrm{GPI} = \left|10^5\eta\right|^{\frac{3}{2}}\left(\frac{\mathrm{RH}}{50}\right)^3\left(\frac{V_{\mathrm{pot}}}{70}\right)^3(1+0.1V_s)^{-2}. \tag{A1}$$

In equation (A1), η is 850 hPa absolute vorticity (s^{-1}), RH is relative humidity (%) at 700 hPa, and V_s is the magnitude of vertical wind shear between 850 hPa and 200 hPa. V_{pot} is the maximum potential intensity as defined in *Emanuel* [1995]:

$$V_{\mathrm{pot}}^2 = C_p(T_s - T_0)\frac{T_s}{T_0}\frac{C_k}{D_D}\left(\ln\theta_s^* - \ln\theta_s\right), \tag{A2}$$

where T_s is the SST and T_0 is the air temperature at tropopause. θ_s^* and θ_s are the surface saturation equivalent potential temperature and equivalent potential temperature, respectively.

Acknowledgments

All data sets used in this study are publicly available: gridded OLR, precipitation, and reanalysis data acquired from NOAA/ESRL/PSD (http://www.esrl.noaa.gov/psd/data/gridded/), gridded surface temperature data acquired from NASA/GISS (http://data.giss.nasa.gov/gistemp/), climate indices (NINO3.4 and AMO) acquired from NOAA/ESRL/PSD (http://www.esrl.noaa.gov/psd/data/climateindices/list/), named Atlantic storm counts acquired from NOAA/NHC (http://www.nhc.noaa.gov/data/#tracks_all), ACE time series acquired from NOAA/HRD (http://www.aoml.noaa.gov/hrd/hurdat/comparison_table.html), NOAA/NHC seasonal predictions acquired from NOAA/CPC (http://www.cpc.ncep.noaa.gov/products/outlooks/hurricane-archive.shtml), CSU seasonal predictions acquired from the CSU Tropical Meteorology Project (http://hurricane.atmos.colostate.edu/forecasts/), and tropical cyclone tracks acquired from HURDAT2 (http://www.nhc.noaa.gov/data/#hurdat). All code and derived data available upon e-mail request to the authors. The authors thank Eric Blake of NOAA/NHC for helpful discussions as this manuscript was being prepared, and Cathy Smith (NOAA/ESRL/PSD) for facilitating the Interpolated OLR data set. The authors also thank Jim Kossin, one anonymous reviewer, and the Editor for constructive comments during peer review. K.B.K. acknowledges support from the Alfred P. Sloan Foundation. L.L. is supported by the Postdoctoral Scholar Program at the Woods Hole Oceanographic Institution, with funding provided by the Ocean and Climate Change Institute. Updated OLR-based predictions will be posted annually at http://www.colorado.edu/oclab/olr.

References

Adler, R. F., et al. (2003), The version 2 Global Precipitation Climatology Project (GPCP) monthly precipitation analysis (1979–present), *J. Hydrometeorol.*, *4*, 1147–1167.

Bell, G. D., and M. Chelliah (2006), Leading tropical modes associated with interannual and multidecadal fluctuations in North Atlantic hurricane activity, *J. Clim.*, *19*, 590–612.

Breiman, L. (2001), Random forests, *Mach. Learn.*, *45*, 5–32.

Dong, B., and R. Sutton (2015), Dominant role of greenhouse gas forcing in the recovery of Sahel rainfall, *Nat. Clim. Change*, *5*, 757–760.

Emanuel, K. A. (1995), Sensitivity of tropical cyclones to surface exchange coefficients and a revised steady-state model incorporating eye dynamics, *J. Atmos. Sci.*, *52*, 3969–3976.

Emanuel, K. A., and D. S. Nolan (2004), Tropical cyclone activity and the global climate system, Preprints, in *26th Conference on Hurricanes and Tropical Meteorology*, pp. 240–241, Am. Meteorol. Soc., Miami, Fla.

Hansen, J., R. Ruedy, M. Sato, and K. Lo (2010), Global surface temperature change, *Rev. Geophys.*, *48*, RG4004, doi:10.1029/2010RG000345.

Hopsch, S. B., C. D. Thorncroft, and K. R. Tyle (2010), Analysis of African easterly wave structures and their role in influencing tropical cyclogenesis, *Mon. Weather Rev.*, *138*(4), 1399–1419.

Hsieh, J.-S., and K. H. Cook (2008), On the instability of the African easterly jet and the generation of African waves: Reversals of the potential vorticity gradient, *J. Atmos. Sci.*, *65*(7), 2130–2151.

Kalnay, E., et al. (1996), The NCEP/NCAR 40-Year Reanalysis Project, *Bull. Am. Meteorol. Soc.*, *77*, 437–471.

Karnauskas, K. B. (2006), The African meridional OLR contrast as a diagnostic for Atlantic tropical cyclone activity and implications for predictability, *Geophys. Res. Lett.*, *33*, L06809, doi:10.1029/2005GL024865.

Karnauskas, K. B., and C. C. Ummenhofer (2014), On the dynamics of the Hadley circulation and subtropical drying, *Clim. Dyn.*, *42*(9–10), 2259–2269.

Landsea, C. W., and J. L. Franklin (2013), Atlantic hurricane database uncertainty and presentation of a new database format, *Mon. Weather Rev.*, *141*, 3576–3592.

Liebmann, B., and C. A. Smith (1996), Description of a complete (interpolated) outgoing longwave radiation dataset, *Bull. Am. Meteorol. Soc.*, *77*, 1275–1277.

Price, C., N. Reicher, and Y. Yair (2015), Do West African thunderstorms predict the intensity of Atlantic hurricanes?, *Geophys. Res. Lett.*, *42*, 2457–2463, doi:10.1002/2014GL062932.

Rodwell, M. J., and B. J. Hoskins (1996), Monsoons and the dynamic of deserts, *Q. J. R. Meteorol. Soc.*, *122*, 1385–1404.

Thorncroft, C., and K. Hodges (2001), African easterly wave variability and its relationship to Atlantic tropical cyclone activity, *J. Clim.*, *14*, 1166–1179.

Zhang, G., and Z. Wang (2013), Interannual variability of the Atlantic Hadley circulation in boreal summer and its impacts on tropical cyclone activity, *J. Clim.*, *26*, 8529–8544.